Vol. 10(1), pp. 1-9, April 2019
DOI: 10.5897/JEEER2018.0624
Article Number: 5517C8560648
ISSN 1993–8225

http://www.academicjournals.org/JEEER

ACADEMIC JOURNALS

Journal of Electrical and Electronics Engineering Research

Full Length Research Paper

Impact of electromagnetic interface of soft magnetic sensor on IoTs current detector: Design and development

Chang-Hung Hsu*, Ann-Shing Chang and Chin-Ping Fung

Department of Mechanical Engineering, Oriental Institute of Technology, New Taipei City 220, Taiwan.

Received 22 September, 2018; Accepted 13 February, 2019

This paper presents the electromagnetic interface (EMI) impact on the current transformer with amorphous HB1-M core, printed circuit board (PCB) power transformer and the filter of inductor for Internet of Things (IoTs) device. According to the antenna principle, the radiation emission power responses of PCB transformer and current transformer are estimated and found to be negligible due to the EMI experimental report. Based on this reason, consideration of the amorphous core in design manufacturing and EMI filter development is indispensable. Thus, the current transformer of amorphous HB1-M core is annealed at 350°C and soaked for 1.5 h. The simulation results of electromagnetic field show an EMI impact on filter performance. EMI frequency between 50 to 400 MHz for filter is found to be suitable for PCB. Experimental results have confirmed that the application of PCB transformer with HB1-M would be performed as well in high permeability and sensitivity.

Key words: Internet of things (IoTs), electromagnetic interface (EMI), soft magnetic sensor.

INTRODUCTION

Internet of things (IoTs) is the network of devices, and recent research proposed a performance degradation of IoTs communications in smart cities by using a new routing algorithm to improve them. This study has figured out an algorithm defined as smart and self-organised routing algorithm (SSRA), which can be selected as the best route for the packets and for which SSRA can be extended to the devices lifetime by parameter of fair and efficient energy consumption (Hamrioui et al., 2018). Due to this reason, the IoTs growing popularity is gaining more attention as the security and sensitivity problem in IoTs device applications and sensor-based threats to IoT devices is developed. A comprehensive survey of IoTs devices with current sensors and sensor management themselves adopted in commodity IoTs system can be obtained (Math´una et al., 2012; Yamaguchi et al., 1993). A common development approach in metering and protective relaying for smart grid and power substations is useful where it facilitates the safe measurement of large currents, often in the presence of high voltages (Brunet et al., 2002). Also, some case in electronic circuit application and minor current signal detection is not only provided typically in signal measurement but it can transmit stable signal by using communication system and support analog-digital signal to enhance receiver to user application (Lu et al., 2010). Actually, development of electronic circuit to surround electromagnetic signal impact on the device is not easily measured.

*Corresponding author. E-mail: chshiu@mail.oit.edu.tw.

The study by Jia et al. (2011) contains useful background information on switching power supplies (SPS) for various fields of application in industrial and commercial environments for driving MOSFETs in switching power supply. The modern trends in industry for maximum power density performance at minimum cost depend on higher power efficiency, and should be considered consistently. Besides, it is well-known that basic principle of SMS is satisfied with several characteristics including fast switching of high current and voltage signals within power converter systems. Electromagnetic interference (EMI) problems become a more critical problem due to the compromise between efficiency and power density (Hui et al., 1999a, b).

It is interesting to discover that because of special theory of relativity, electric and magnetic fields are two aspects of the same phenomenon depending on a chosen reference device structure of observation; also, the printed circuit board (PCB) with magnetic core device performed SPS induced significant EMI source which faces their intrinsic switching properties and the generated EMI noise levels. Moreover, electromagnetic compatibility (EMC) regulations need to satisfy the following rules, for example, line-current harmonic standards and IEC 61000-3-2 (Orlando et al., 2006). Once the electronic device from customer meets these standards, it should then be considered that the different EMI mitigation and harmonic line current reduction techniques for preventing damage of product design is significantly important (Hui et al., 1999a). Besides, EMC analysis represents an important step of the overall SMS design procedure to assure both low EMI emission and high power quality.

Regarding the current and voltage sensing in power electronic converters (Beghou and Costa, 2018), it has been demonstrated that the converter in electromagnetic interference is associated with an electromagnetic field characterization analysis by using the inverse Fourier transform method. It has combined two structures with a circuit analysis that enable prediction of the necessary parameters to be achieved with the current programmed to control the chosen parameters. Another research in new integration circuit (IC) development (Lin et al., 2017), has successfully proposed an improved method upon the probe structure specified with IEC 61967-4 standards to measure the convenience noise from IC pins. The magnetic field probe, TEM cell, and CISPR 22 showed limitation only at a 10 meter far-field distance measured environment used to make a comparative analysis and to verify the practicality of the improved probe. The common-mode (CM) LC modules and difference-mode (DM) modules of the planner EMI filter are presented (Wang and Xu, 2014). The electrostatic field model and the harmonic magnetic field model of these modules are established, respectively. The inductance and resistance depending on experimental results are shown to be very closely related to frequency. Thus, consideration of the skin effect of the conductors and the eddy current loss of the magnetic core can be measured. Also, both the DM and CM inductance in leakage layer are very small, independent of frequency and can be validated.

However, aforementioned discussion for power station with IoTs device in running a more stable quality signal transmission under EMC/EMI has not yet been fully explored. This paper is organized as follows. The characteristics of soft material with amorphous core HB1-M, and EMI absorber of variable resistor (also named as varistor) is introduced in Section II. Experimentation results is discussed in Section III and Conclusions is introduced in Section IV.

MATERIAL PROPERTY AND EMI FILTER DESIGN SIMULATION

High sensitivity soft core with amorphous HB1-M

Amorphous alloy with HB1-M and SA1 is made by Hitachi company in Japan. In this product, the physical characteristics include HB1-M and SA1 with thicknesses of 0.025 μm and widths of 20 mm. Besides, both magnetic cores annealed at 320°C (for HB1-M) and 350°C (for SA1), and was soaked for around 1.5 h. According to a previous research (Hsu et al., 2013), amorphous magnetic properties during crystalline, re-crystalline phase and microstructure surface, are detected by using vibrating sample magnetometer (VSM) and X-ray diffraction (XRD). In Figure 1a, it is shown that a vibrating-sample magnetometer (VSM) used to measure magnetic properties of soft material such as amorphous alloy include parameters of saturation magnetic induction $\mathrm{B_s}$ corecovity $\mathrm{M_r}$ and magnetic remanence $\mathrm{B_r}$, respectively. B-H curve or hysteresis loop happen because an external magnetic field was applied to a ferromagnetic material such as amorphous alloy or silicon steel and the material atomic dipoles will align themselves with it. VSM is used to measure the hysteresis loop, thus becoming a very simple and fast method to characterize magnetic materials. The hysteresis curves and their properties B_s, M_r, and B_r indicates the point of view. The B-H loops at room temperature of the investigated alloy Hitachi Co, amorphous alloy SA1 and HB1-M were measured at a constant frequency ($f = 1kHz$), and the results are presented in Figure 1a.

By using XRD, the crystallization behavior effects on magnetic property of Fe–based amorphous alloys were studied. In Figure 1b, X-ray diffraction (XRD) measurement is a method to investigate microscopic properties, such as crystal structure, orientation and deformation. Generally, this study has carried out the $\alpha - F_e$ and $\gamma - F_e$ structure in amorphous alloy during and after the annealing procedure to validate the soft magnetic properties of the sensor cores.

Also, in Figure 1c, the scanning electron microscopy (SEM) and energy dispersive spectroscopy (EDS) are equipment for detecting chemical elemental composition and mapping material components. The SEM/EDS microscope system can be used for examining amorphous material in micro-scale or nano-scale features where it can be magnified into macro-vision up to 300,000x and to detect chemical composition in or on the surface of amorphous material sample. Then the amorphorous magnetic sensor structure can be shown as in Figure 2.

Design of EMI filter and FEA simulation

EMI noise sources within power-line or radiation emission of

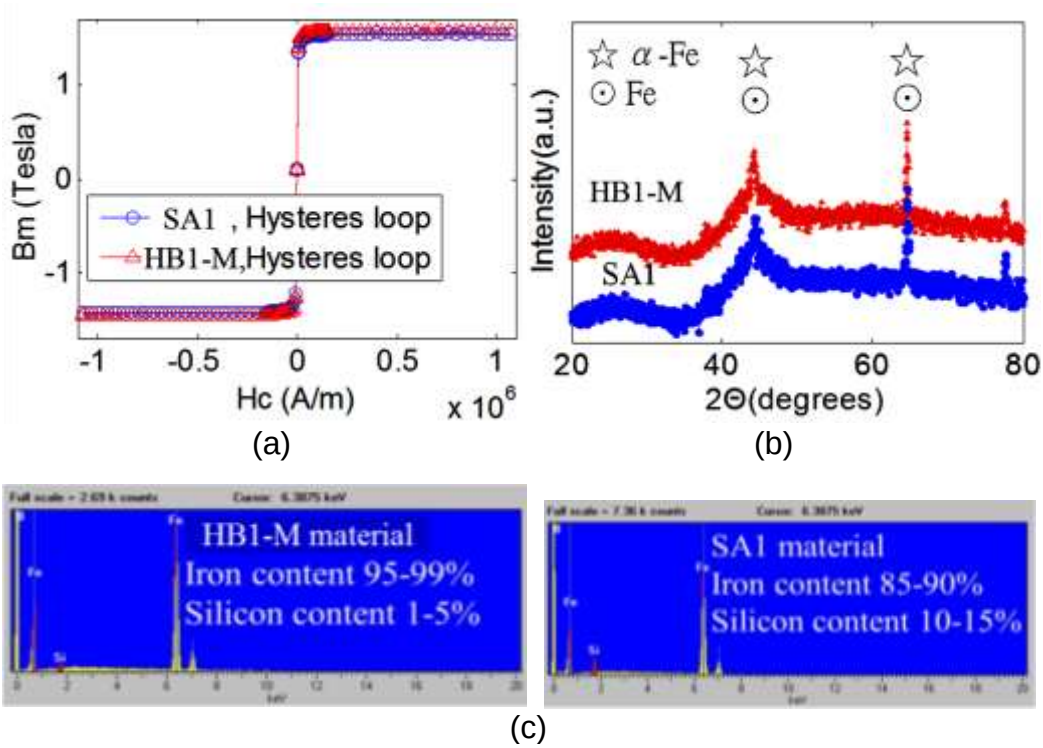

Figure 1. The measured results of the magnetic properties for amorphous materials HB1-M and SA1: (a) VSM, (b) XRD and (c) EDS.

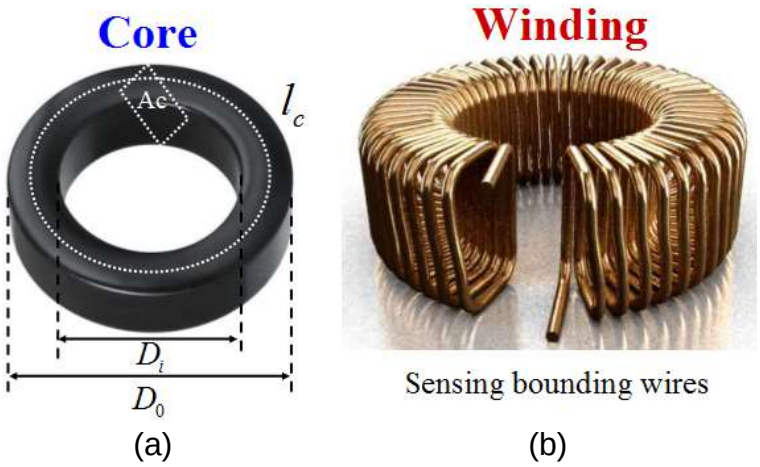

Figure 2. Sensing magnetic core device, amorphous HB1-M material: (a) core, (b) winding.

antenna equipment, operated at duty cycle characteristic of currents is made. The critical PCB continuously turning loops (di/dt) and the pulsating voltages of the phase nodes (dv/dt) are defined. The common (CM) and differential (DM) noise sources as well as the corresponding noise propagation paths are shown in Figure 3.

According to the aforementioned discussion, the power system with communication PCB device for varistors within EMI filter function has been considered. The design of practical EMI filter of varistors is based on the selection of an appropriate core and winding configuration. The varistor need to withstand the rated current without saturating while simultaneously providing the required CM/DM noise attenuation. The core of varistor is chosen from a typical material. Also, the permeability curves $\mu r(f)$ is

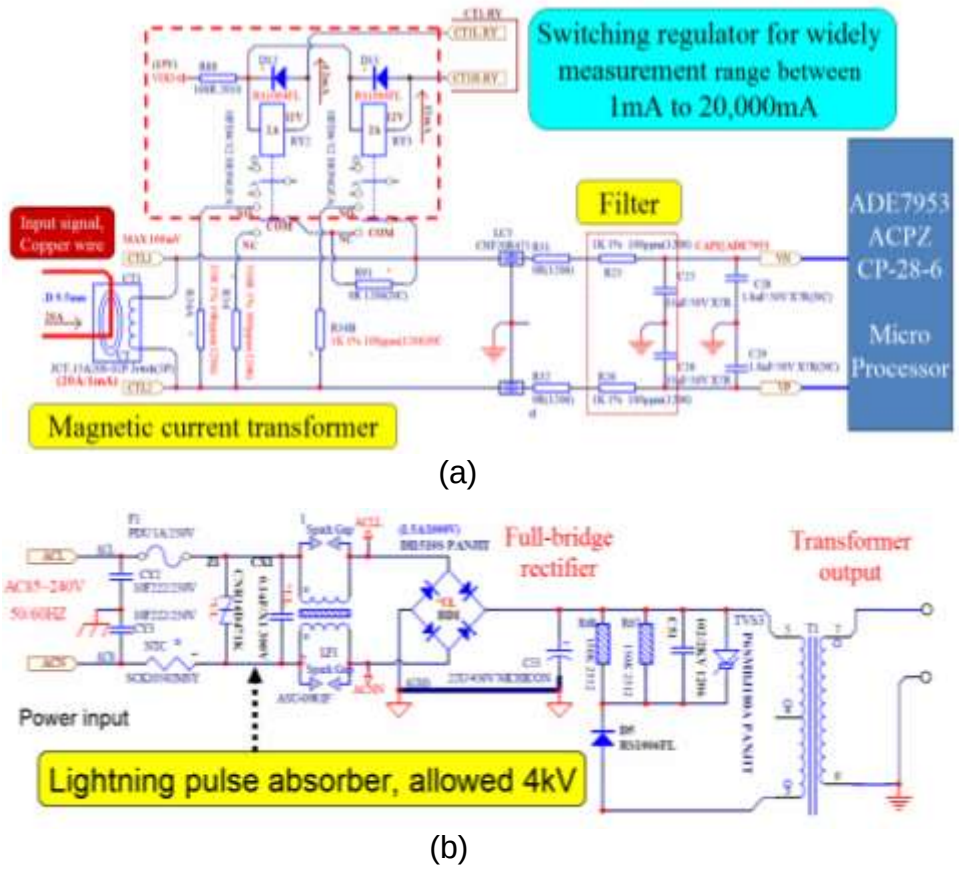

Figure 3. Magnetic core and electronic circuit: (a) CT and wide-raged switching, (b) lightning pulse absorber.

referred to by datasheets or impedance measurements.

EMI analysis is performed as follows: firstly, EMI noise sources is defined, including identifying fast rates of change of currents di/dt and voltages dv/dt. Next, focus should be on noise propagation paths, like CM/DM conduction paths. Then, most important effort is put on design of an EMI filter. PCB identification should be performed in areas of occurring higher frequencies and more than a few MHz, leading to unwanted electromagnetic behavior. Before that step, it is well-known that numerical techniques for power varistor and electronics component applications are simulated by finite element analysis (FEA) as shown in Figure 4.

The finite element analysis (FEA) is a numerical method for solving engineering problems. For this reason, it can be deal for typical problems that include electromagnetic potential, heat transfer, structural analysis, fluid flow and mass transport,

Consideration of emission radiation

The current transformer with amorphous core in dimension of shape is made by higher permeability and magnetic flux density of HB1-M. The transformer winding for each wire turn can be regarded as a loop antenna response. Next, to simplify the radiation from the outermost turn, the radiation range is only around radius of 15 mm. It should be noted that the radiation efficiency and average radiated power increase with the radius of a loop antenna is considered. Once the current flows in the loop at an angular frequency, it can be

respectively. So, this method can be used generally in resolving the above-mentioned and boundary value problems for partial differential equations. Figure 4 revealed that the varistor component under electrical potential situation is simulated by FEA, which include results on model edge, electric field by slice, iso-surface, FEA boundary, electric field arrow, and electric field streamline, respectively. It can be shown that the surge absorber is used as resistant to the surge wave from power source impact on PCB circuit. From the FEA results, positive and negative charges can be arranged in space for easy viewing of the simulated result for electric field and electrostatic potential of the variable resistance performance. It can be used for observing and plotting of equipotential lines, and also discovering their electric field variable conditions which apply to the varistor in resistance surge wave from power line under operation frequency situation.

expected that the energy in the air should be affected by radiation response. The radiation intensity is expressed as follows (Lee, 1984:

$$\mathrm{U}(\theta) = \frac{\eta}{2}\left(\frac{kI_o a}{4\pi}\right)^2 sin^2\theta \quad (1)$$

where I_o is the current in the loop; η is intrinsic impedance of the medium, with $\eta = \sqrt{\mu/\epsilon} = k/\omega\epsilon$; k is defined as $\omega/c = 2\pi/\lambda$; a is the radius of the loop; c is speed of light $(3 \times 10^8\, m/s)$; and θ is radiation angle. Then, the operation frequency for radiated power is expressed as follow.

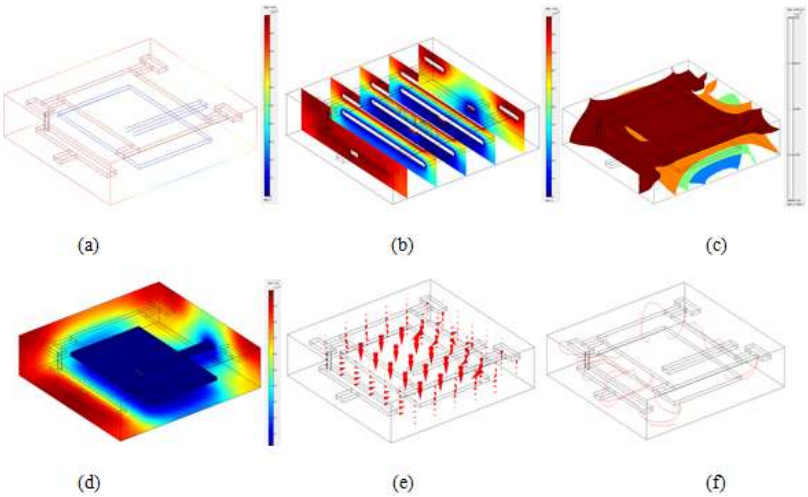

Figure 4. The FEA simulated results of electrical potential for varistor: (a) model edge, (b) electric field by slice, (c) iso-surface, (d) FEA boundary, (e) electric field arrow, and (f) electric field streamline.

$$\mathrm{P} = 160\pi^6 I_o^2 \left(\frac{f_c a}{\lambda}\right)^4 \quad (2)$$

It can be shown that the above formula for radiated power depends on several parameters like the current I_o, power of the operation, the dimension, radius a of the structure and the operating frequency f_c . The radiated power drastically increases with increasing frequency and the dimension of the radiating structure. According to the antenna principle, if the loop radiator have a good response due to a radius dimension, this is the order of magnitude close to the wavelength of the radiated signal.

EXPERIMENTAL AND SIMULATION RESULTS

This study has revealed that reduction of the emission noise result on PCB can be simulated by FEA and measured through experiments based on the alternating current power lines with various types of noise. Then, when the voltage level and rise time causes the noise, it will induce noise impact on PCB device by three signals from power line. First, a higher frequency noise that mainly consist of the harmonic components of high frequencies switching device. Further, EMI noise is induced by switching noise to impact voltage level with relatively lower value from mV to tens of mV and higher. Another problem is the impulsive noise. It will generate that noise due to the switching time or motor devices. Usually, voltage level reaching around several thousand voltages could be generated. For surge noise, lightning impulse produces larger amount of energy as well as very high voltage and current. The peak voltage may reach several tens of kV due to power line that usually generated that surge condition.

In this study, amorphous wound cores are applied in analog signal receiver position. Actually, there are many applications in power supplies, like high frequency Inverters or UPS for more effective noise suppression function caused by rapidly switching changes in current. Due to this reason, higher permeability of amorphous cores can allow for an excellent performance in the suppression of reversely recovery current signal from the on-off switching power or surge current from measurement environments. It is well-known that the saturation magnetic flux density is twice as high as Fe-based amorphous material than that of traditional silicon steel material. It can be summarized as two factors with higher pulse permeability and lower core loss that are comparable to other iron steel. Based on this, Fe-based amorphous core can offer higher performance in suppression of surge current and voltage.

Regarding soft core operation on EMI environment, it can be seen that PCB transformer with amorphous magnetic core in power electronic circuits is addressed. Figure 5a shows that the FEA simulation results of RF wave are shielded by metal material. It supports a concept for design consideration of the IoTs container. Also, emission testing environment and shield of IoTs device is shown in Figure 5b which displays an exact experimental environment having a high energy emission from antenna device. Besides, the definition of electromagnetic interference (EMI) or radio-frequency interference (RFI) is for radio frequency spectrum under a disturbance generated by an external source that affects an electrical circuit due to the electromagnetic induction, electrostatic coupling, or conducted situation. This disturbance (noise) might affect the performance of the circuit or could stop the device operation at normal function. EMI problem can emanate from man-made and natural sources that generate changing electrical currents and voltages. Significantly, the EMI noise can be caused

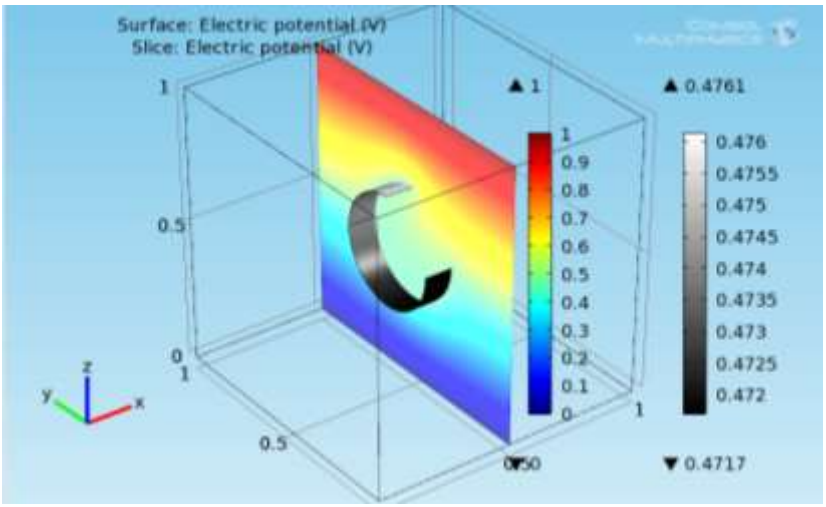

(a)

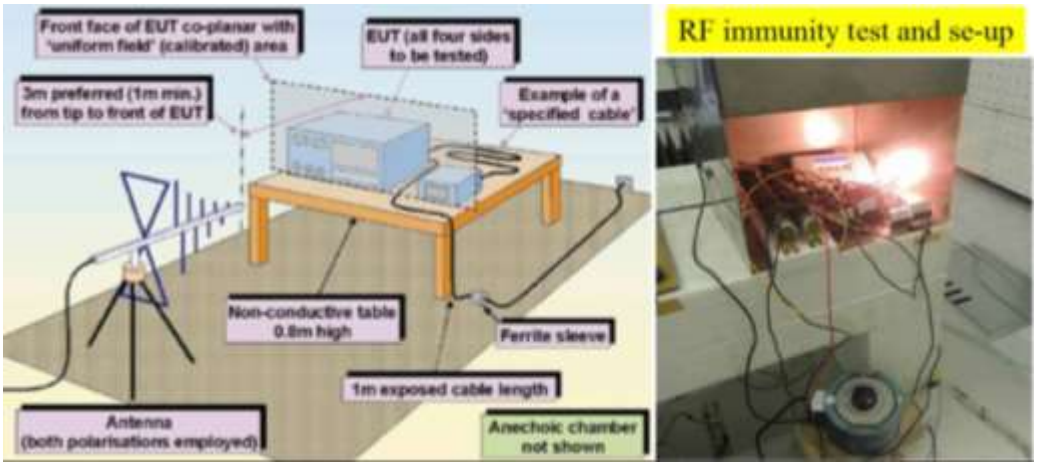

(b)

Figure 5. RF testing and environment set-up: (a) RFCT and wide-ranged switching, (b) emission testing environment and shield of IoTs device.

by many factors including lightning, solar flares, ignition systems, and mobile phones, respectively.

Thus, the EMI conducted interference is organized as follow: the first is for conducted EMI caused by the physical contact of the conductors as opposed to radiated EMI which can be caused by induction due to no more physical contact of the conductors. By radiation emission, lower frequencies of the EMI are caused by conductors at higher frequencies. Also, the EMI can through the ground wire affect an electrical facility directly. In this study, EMI test follows the International Electrotechnical Commission (IEC) standard 61000 to perform the testing procedure and also satisfactorily operate at frequencies between 50 to 400 MHz.

Therefore, according to the antenna principle, the performed EMC/EMI experiment indicates that the PCB transformer with amorphous core under consideration showed a radius much smaller than that of the wavelength of the operating frequency. Due to the original property of amorphous core, it is understood that lower coercivity, higher permeability and magnetic flux density compared with traditional silicon steel core can be used to prevent electrical pollution of EMI affecting the response of the magnetic sensing winding can be obtained.

Thus, the current transformer sensing winding extends a worse transmitting signal that is received from an outside antenna signal, with both signals radiated power energy that can be negligible, in this case, the EMI experimental results as shown in Figure 6. Here, the testing results are passed since it performed under 50 to 400 MHz and below standard of 50 $dB\mu V/m$. For conducted emission results, it can be seen that the measurement results falls between operation frequency of 0.15 to 21.5 MHz, that is, around 37 $dB\mu V/m$ which is

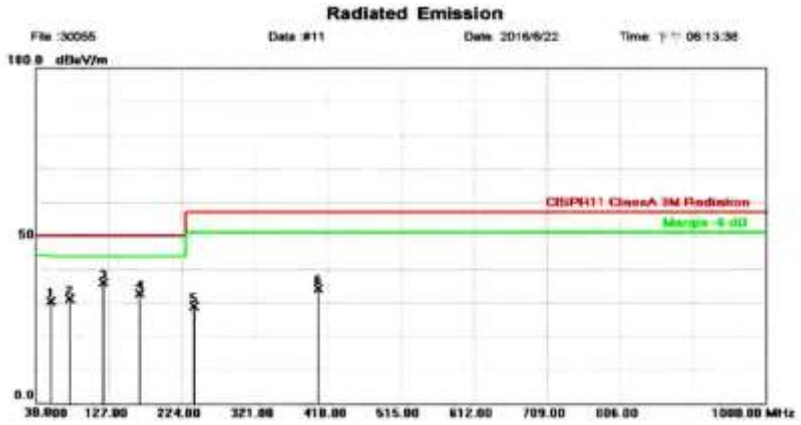

No.	Mk.	Freq	Reading Level	Correct Factor	Measure-ment	Limit	Over		
		MHz	dBuV	dB	dBuV/m	dBuV/m	dB	Detector	Comment
1		50.3700	46.10	-15.74	30.36	50.00	-19.64	QP	
2		74.6200	50.30	-19.29	31.01	50.00	-18.99	QP	
3	*	115.2400	54.10	-18.27	35.83	50.00	-14.17	QP	
4		167.7400	48.20	-15.66	32.54	50.00	-17.46	QP	
5		239.5200	43.60	-16.73	26.87	57.00	-30.13	QP	
6		405.3900	45.70	-11.51	34.19	57.00	-22.81	QP	

(a)

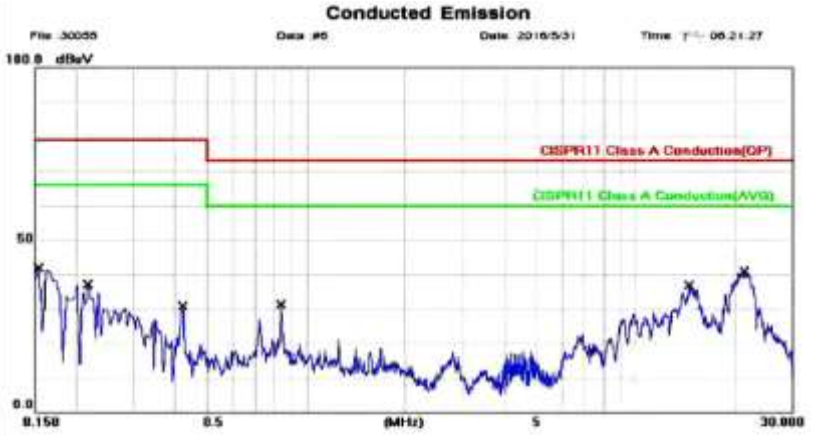

No.	Mk.	Freq.	Reading Level	Correct Factor	Measure-ment	Limit	Over		
		MHz	dBuV	dB	dBuV	dBuV	dB	Detector	Comment
1		0.1540	36.20	0.07	36.27	79.00	-42.73	QP	
2		0.2180	32.00	0.08	32.08	79.00	-46.92	QP	
3		0.4220	29.40	0.10	29.50	79.00	-49.50	QP	
4		0.8420	29.40	0.11	29.51	73.00	-43.49	QP	
5		14.5660	31.30	0.41	31.71	73.00	-41.29	QP	
6	*	21.5420	37.40	0.46	37.86	73.00	-35.14	QP	

(b)

Figure 6. Emission testing results: (a) radiated emission, (b) conducted emission.

lower than the standard of 73 $dB\mathrm{uV/m}$.

From Equations (1)-(2) experimental result in case of conducting paths of the electronic circuit, the device of PCB power transformer shows a smaller switching transient impact response due to the measurement results obtained. Therefore, it can be shown that the emission radiation signal of EMI from IoTs device is not significant. Field measurements of the entire power circuit have confirmed that the coreless PCB transformer is not a major EMI source; at least, it did not generate the EMI

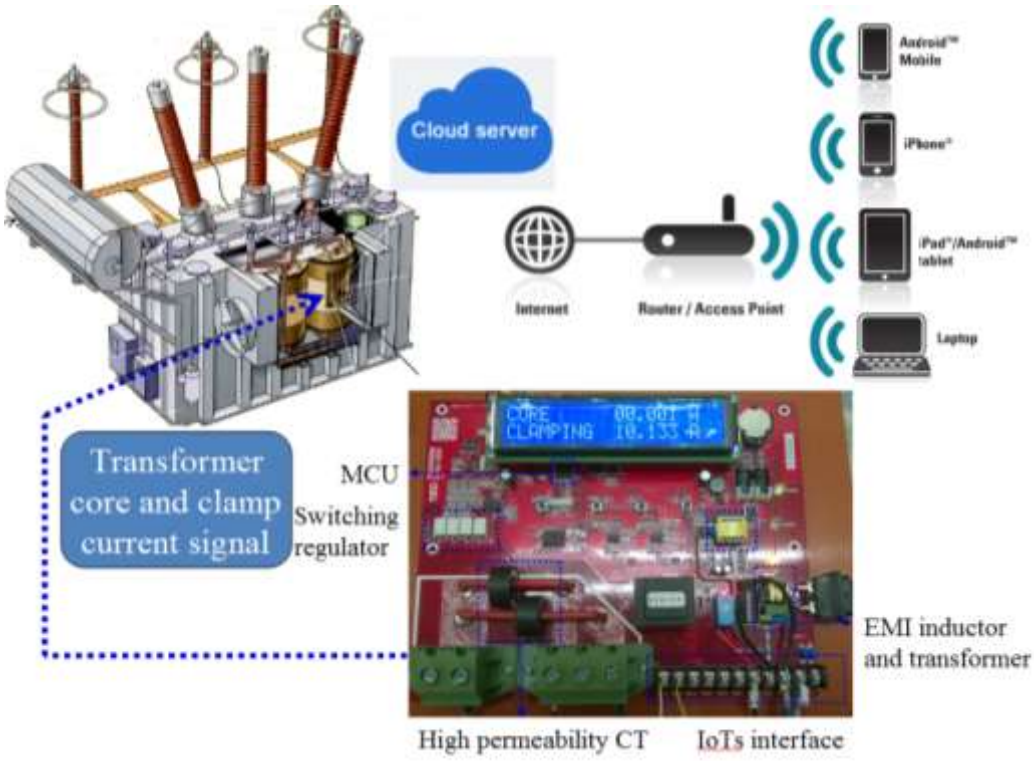

Figure 7. Installation of IoTs device, with current transformer sensing connected with cloud server and also with three-phase power transformer.

signal by itself. Both theoretical evaluation and experimental results indicate that the application of IoTs device in PCB transformer and sensing magnetic core can be suitable in power system. Finally, application of IoTs device within one of three-phase power transformer equipment, including detection, transfer signal, alternating signal converted by AC and DC, alongside cloud server to storage signal is shown in Figure 7.

Conclusion

This paper presents the EMI impact on the current transformer with amorphous HB1-M core, printed circuit board (PCB) power transformer and EMI filter of varistor for Internet of Things (IoTs) device. According to the antenna principle, the radiation emission power responses of PCB transformer and current transformer are estimated and found to be negligible due to the experimental report of EMI. The major radiated EMI source in the frequency range between 50 to 400 MHz is found to be the filter of the power circuit, where antenna emission energy transients occur, rather than the PCB transformer. Experimental results have confirmed that the application of PCB transformer in electronic circuit might not be seriously an EMI problem on the power electronic circuit.

ACKNOWLEDGEMENTS

The authors thank Mr. Yi-Chen (Ithen) Hsu, who is with the CEO of Fortune Electric Company (Taiwan) for charging and supporting the research work. Besides, the authors also appreciate the funding support from MOST (No: 107-2218-E-161-001) Republic of China (R.O.C.) in Taiwan 2018.

CONFLICT OF INTERESTS

The authors have not declared any conflict of interests.

REFERENCES

Brunet M, O'Donnell T, Baud L, Wang N, O'Brien J, McCloskey P, O'Mathuna SC (2002). Electrical performance of microtransformers for DC-DC converter applications. IEEE Transactions on Magnetic 38(5):3174-3176.

Hamrioui SS, Hamrioui CAM, Jaime L, Pascal L (2018). Smart and self-organised routing algorithm for efficient IoT communications in smart citie. IET Wireless Sensor Systems 8(6):305-312.

Hsu C-H, Chun-Yao L, Yeong-Hwa C, Faa-Jeng L, Chao-Ming F, Lin J-

G (2013). Effect of magnetostriction on the core loss, noise, and vibration of fluxgate sensor composed of amorphous materials. IEEE Transactions on Magnetic 49(7):3862-3865.
Hui SY, Henry S-HC, Tang SC (1999a). Coreless PCB-based transformers for power MOSFETS/IGBT gate drive circuits. IEEE Transactions on Power Electronic 14(3):442-430.
Hui S-YR, Tang SC, Chung H (1999b). Optimal operation of coreless PCB transformer-isolated gate drive circuits with wide switching frequency range. IEEE Transactions on Power Electronic 14:506-514.
Lu J, Jia XW, Padmanabhan K, Hurley WG, Shen ZJ (2010). Modeling, design, and characterization of multiturn bondwire varistors with ferrite epoxy glob cores for power supply system-on-chip or systemin-package applications. IEEE Transactions on Power Electronic 25(8):2010-2017.
Jia H, Lu J, Wang X, Padmanabhan K, Shen ZJ (2011). Integration of a monolithic buck converter power IC and bondwire varistors with ferrite epoxy glob cores. IEEE Transactions on Power Electronic 26(6):1627-1630.
Lee KF (1984). Principles of Antenna Theory. New York: Wiley.
Lin H-N, Hung-Chi C, Chung-Wei K, Yen-Tang C (2017). Design and application of a mobile miniature current probe for analysing the cause of EMI noise in IC circuits. IET Science, Measurement and Technology 11(5):655-665.
Beghou L, Costa F (2018). EMI-Based current and voltage sensing for the control of power electronic converters. IEEE Transactions on Circuits and Systems II: Express Briefs 65(7):918-922.
Math´una CO, Wang N, Kulkarni S, Roy S (2012). Review of integrated magnetics for power supply on chip (PwrSoC). IEEE Transactions on Power Electronic, 27(11):4799-4816.
Orlando B, Hida R, Cuchet R, Audoin M, Viala B, Pellissier-Tanon D, Gagnard X, Ancey P (2006). Low-resistance integrated toroidal varistor for power management. IEEE Transactions on Magnetic 42(10):3374-3376.
Wang S, Xu C (2014). Extraction of magnetic parameters for elements of a planar EMI filter. IEEE Transactions on Electromagnetic Compatibility 56(2):360-366.
Yamaguchi K, Ohnuma S, Imagawa T, Toriu J, Matsuki H, Murakami K (1993). Characteristics of a thin film microtransformer with circular spiral coils. IEEE Transactions on Magnetic 29:2232-2237.